# International Conference on Space Optics—ICSO 2010

Rhodes Island, Greece

4–8 October 2010

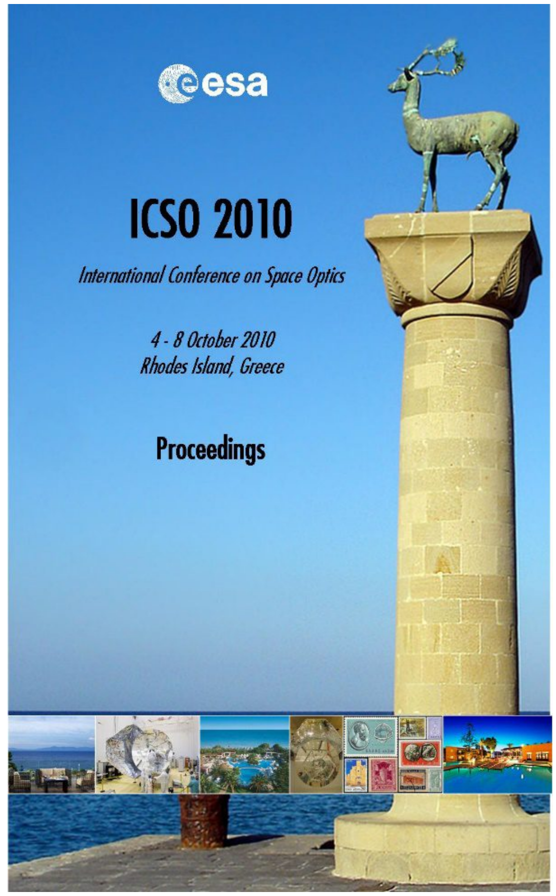


*Edited by Errico Armandillo, Bruno Cugny, and Nikos Karafolas*

## *The SPICA Telescope: design evolution and expected performance*

*L. M. Gaspar Venancio, D. Doyle, K. Isaak, T. Onaka, et al.*

International Conference on Space Optics — ICSO 2010, edited by Errico Armandillo, Bruno Cugny, Nikos Karafolas, Proc. of SPIE Vol. 10565, 1056555 · © 2010 ESA and CNES
CCC code: 0277-786X/17/$18 · doi: 10.1117/12.2309162

# THE SPICA TELESCOPE: DESIGN EVOLUTION AND EXPECTED PERFORMANCE

L.M. Gaspar Venancio[1], D. Doyle[1], K. Isaak[1], T.Onaka[2], H. Kaneda[3], T. Nakagawa[4], H. Matsuhara[4], N. Takahashi[4], T. Yamawaki[5]
[1]*European Space Agency/ESTEC, Keplerlaan 1, 2200 AG, Noordwijk ZH, The Netherlands.*
*(luis.miguel.gaspar.venancio, dominic.doyle, kate.isaak)@esa.int*
[2]*University of Tokyo, 7-3-1 Hongo, Bunkyo-ku, Tokyo, 113-0033, Japan.*
*onaka@astron.s.u-tokyo.ac.jp*
[3]*Nagoya University, Furo-cho, Chikusa-ku, Nagoya, Aichi, 464-8602, Japan.*
*kaneda@u.phys.nagoya-u.ac.jp*
[4]*Japanese Aerospace Exploration Agency, 3-1-1 Yoshinodai, Chuo-ku, Sagamihara, Kanagawa, 252-5210, Japan.*
*nakagawa@ir.isas.jaxa.jp, maruma@ir.isas.jaxa.jp, takahashi.nobuhiro2@jaxa.jp*
[5]*Japanese Aerospace Exploration Agency, 2-1-1 Sengen, Tsukuba, Ibaraki, 305-8505, Japan.*
*yamawaki.toshihiko@jaxa.jp*

## I. ABSTRACT:

The fairing of the launcher selected for the Space Infrared telescope for Cosmology and Astrophysics (SPICA) mission is not compatible with a primary mirror of 3.5m in diameter. Thus three alternative optical designs of the SPICA Telescope Assembly (STA) with a primary mirror of reduced size were defined and their theoretical optical performances assessed. The impact of the size reduction on the STA optical performances was then quantified. Based on the results of the study, we defined a STA optical design optimum in terms of optical performances and of accommodation of instruments in the STA focal surface.

## II. INTRODUCTION:

The SPace Infrared telescope for Cosmology and Astrophysics (SPICA) mission was selected in October 2007 as a candidate M-class mission for the European Space Agency (ESA) Cosmic Vision 2015-2025 Plan, with the character of "mission of opportunity" [1]. SPICA is led by the Japanese Aerospace Exploration Agency (JAXA) with ESA as a mission partner. It is one of the next generation of large actively cooled cryogenic Space telescopes that will perform observations in the mid and Far Infra Red (FIR) wavelength range. It builds directly on the success of the ESA Herschel telescope and provides spectral overlap in observation capability between Herschel and the forthcoming James Web Space Telescope.

The intended contribution of ESA to the SPICA mission, subject to the Cosmic Vision 2015-2025 down-selection process, includes the procurement of the SPICA Telescope Assembly (STA), the interface management to JAXA of the European instrument SAFARI, collaboration on science operations and possible contributions to the mission ground segment. The SAFARI instrument itself is to be procured by ESA from an European Consortium.

The STA is a 3-meter class Ritchey-Chrétien design which is optimized for the 5 to 210 μm spectral range and operating at a very low cryogenic temperature to ensure sensitivity for very faint Infra Red (IR) sources, and such that FIR instrument performance is limited only by the background radiation from the sky itself. The secondary mirror is foreseen to have refocusing capabilities. Fig. 1 shows the optical configuration for the STA.

The physical diameter of the primary mirror (M1) of the STA was originally foreseen to be 3.5 meters. Following a cost reduction exercise an alternative launcher was selected. The new launcher fairing volume does not allow a primary mirror larger than 3.2 meters and necessitates a reduction in the primary mirror (M1) to secondary mirror (M2) spacing. The purpose of the work presented here was to define and assess the theoretical performances of alternative designs implementing the reduction in size of M1 and allowing the integration of several Focal Plane Instruments (FPI) sharing the Field Of View (FOV) of the STA. Furthermore, the question of the position of the STA exit pupil was also studied. Finally, as an outcome of the study, an optical design for the STA was defined as baseline for further study.

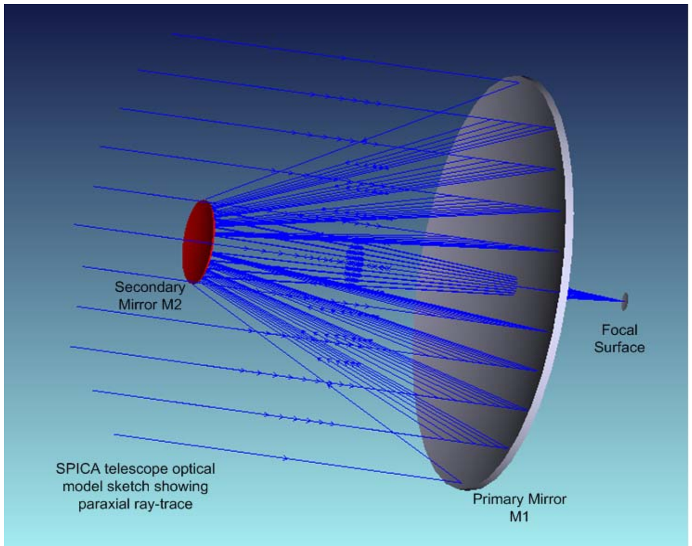


**Fig. 1.** STA optical design configuration and ray trace sketch. For clarity only on-axis rays are shown.

## III. DESIGN OF THE TELESCOPE:

### *A. Design methodology*

The design constraints given in Table 1 are used for the design. The 3rd order aberrations equations governing the Ritchey-Chrétien telescope combination [2] are used to derive the main parameters (radius of curvature and conic constant) defining the shape of the optical surface of the mirrors M1 and M2. From these parameters are derived the Back Focal Length (BFL) of the STA and radius of curvature ($R_{focal}$) of the STA focal surface. However, the values of the parameters obtained with the equations in [2] only accounts for the correction of aberrations up to the 3rd order. Thus, in order to minimize the Wave Front Error (WFE) over the entire field of view, the conic constants of the mirrors and $R_{focal}$ are optimized with the commercial software ZEMAX®. The optimization process has an impact on $R_{focal}$ but not on the BFL. As shown in Fig. 1, the range of the M1 focal length (f1) is limited only by the BFL range. The allowable values for f1 are respectively between 3180.22 mm and 3238.45 mm, the limits being fixed by the maximum allowable volume for the STA and the minimum value of the BFL (898 mm) needed to accommodate the FPI SAFARI.

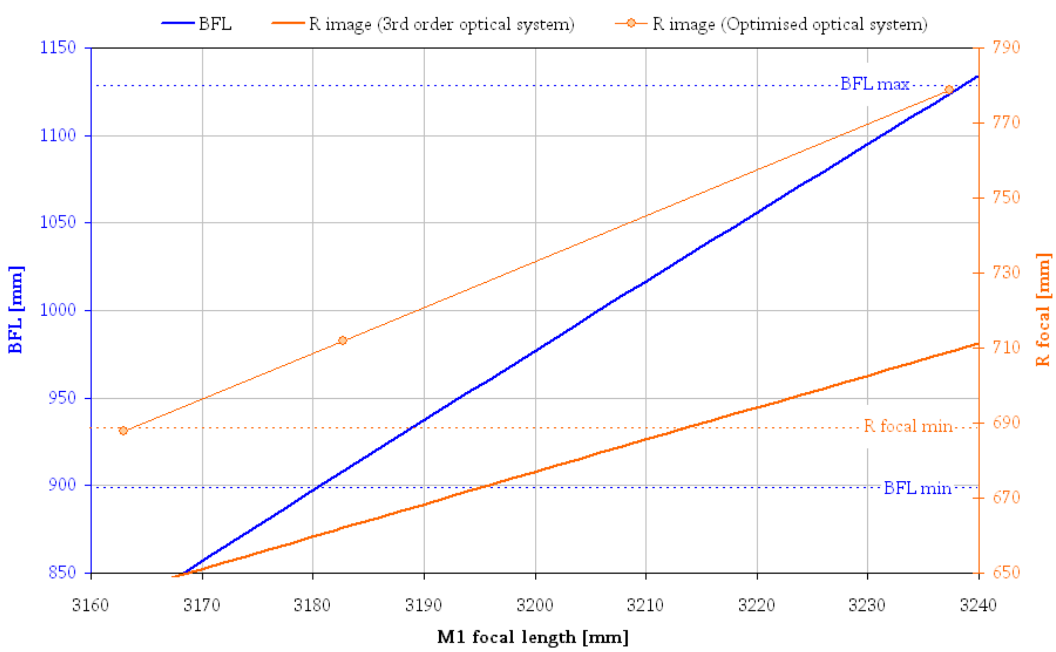


**Fig. 2.** BFL and $R_{focal}$ vs. the focal length of the primary mirror.

**Table 1.** STA design constraints

| | |
|---|---|
| Maximum Back Focal Length ($BFL_{max}$) | 1128 mm |
| Minimum Back Focal Length ($BFL_{min}$) | 898 mm |
| Focal surface radius of curvature ($R_{focal}$) | > 688.5 mm |
| Focal surface conic constant | -1 |
| M1 maximum clear aperture diameter (M1 CAD) | 3.1 m |
| M1 maximum outer physical diameter | 3.2 m (M1 CAD + 100 mm margin) |
| Mirrors spacing | 2511 mm |
| Spectral range | 5 µm to 210 µm |
| Field of view (FOV) without vignetting | ±15 arcmin |
| Imaging quality | Diffraction limited at 5µm over ±5 arcmin<br>Diffraction limited at 30µm over ±10 arcmin |
| Focal length | 16200 mm |

*B. Performance metrics*

The assessment of the STA performance includes the mirror manufacturability evaluated with the dh [4,5] and tool size [3] criteria. The dh criterion, also referred to as Mercier's criterion, is commonly used to assess the manufacturability of optical aspheric surfaces. The Tool Size Criterion (TSC) was developed by the company SESO. It is a measure of the polishing tool size required to achieve the specified optical surface quality. For its calculation the WFE for each mirror is set to 121 nm driven by the diffraction limit at wavelength $\lambda = 5$ µm.

The paraxial Entrance Pupil Diameter (EPD) is also considered as it drives the optical throughput of the STA. The Obscuration Factor (OF) due to the Clear Aperture Diameter (CAD) $D_2$ of M2 is also a contributor to the optical throughput of the STA. The OF is defined simply as the square of the ratio of $D_2$ by the EPD.

Finally the optical interfaces and image quality are assessed with $R_{focal}$, the WFE Root Mean Square (RMS), and the Full Width at Half Maximum (FWHM) of the monochromatic Point Spread Function (PSF). The last two metrics are calculated for the wavelengths and position in the FOV as specified in Table 1. The FWHM is derived from the fit of the PSF with a non-normalized 2-Dimensions (2D) Gaussian function.

*C. Cases of study*

The main design drivers under scrutiny are the BFL and the system stop position which determines the position of the STA exit pupil. In addition to the STA optical design proposed in [1], three different cases are studied. For each case the optical system is optimized in order to minimize the WFE over the entire FOV.

The STA original optical design is referred to as Case 1. The additional cases of study comply with the constraints in Table 1. They are representative of the size reduction of M1. The comparison of Cases 2 and 3 is aimed to evaluate the changes in the performance metrics when changing the BFL. The Case 4 is compared to Case 3 to evaluate the impact on performance metrics of the position of the system stop.

Table 2 summarizes the main characteristics of each case of study.

**Table 2.** Description of the Cases of study

| | **Case 1** | **Case 2** | **Case 3** | **Case 4** |
|---|---|---|---|---|
| M1 CAD [mm] | 3450 | 3100 | 3100 | 3100 |
| Focal length [mm] | 20000 | 16200 | 16200 | 16200 |
| BFL [mm] | 828 | 1128 | 898 | 898 |
| Stop position | M2 | M2 | M2 | M1 |

IV. RESULTS AND DISCUSSION:

The values obtained for the four different cases are summarized in Table 3. The four optical prescriptions of the STA are shown in Table 4.

For all cases the calculated RMS WFEs are lower than the limit given by the Marechal's criterion for diffraction limited optical systems. At a wavelength $\lambda$ = 5 μm the limit is 373 nm RMS and for $\lambda$ = 30 μm the limit is 2236 μm. Also for all cases, the derived PSF FWHM is smaller than the FWHM calculated directly from the theoretical on-axis Airy pattern. This because the amplitude of the 2D Gaussian function used for the fit is not fixed to the maximum value of the PSF thus leading to a small bias in the FWHM. This bias has no impact on the conclusions.

The comparison of Case 1 with Cases 2 and 3 shows that the reduction of M1 size results mainly in an increase of the OF and a smaller EPD. The others performance metrics are not significantly changed except for the PSF FWHM; this is expected, since the f-number of the STA is larger in Case 1 than in Cases 2 and 3. Fig. 3 shows the optical configuration differences between Case 1 and Case 3.

When comparing the Cases 2 and 3, we can deduce that the increase of the BFL has little or no impact on either the imaging quality of the STA or the mirrors manufacturability. The main effects are a 13% increase of the OF, due to an increase of the M2 CAD, and an increase of $R_{focal}$. For large values of the BFL, the increase of $R_{focal}$ may ease the design of the FPIs and their alignment with respect to the STA but at the cost of an increase of the EPD obscuration.

The change of the stop position in Case 4 with respect to Case 3 has almost no impact on either the imaging quality or the mirrors manufacturability. A slight increase in the OF is seen and the EPD is also increased. In contrast to Cases 1, 2 and 3, the STA exit pupil is not physically accessible and can not be used by the FPIs as a "cold stop".

**Table 3.** Summary of the performance metrics. $\lambda$ is the wavelength.

| | | **Case1** | **Case 2** | **Case 3** | **Case 4** |
|---|---|---|---|---|---|
| EPD [mm] | | 3312 | 3000 | 2994 | 3100 |
| Mercier [μm] | M1 | 9.6 | 8.9 | 8.5 | 8.5 |
| | M2 | 8.7 | 7.7 | 7.4 | 6.0 |
| TSC [mm] | M1 | 8.3 | 7.6 | 7.4 | 7.4 |
| | M2 | 3.5 | 3.4 | 3.2 | 3.0 |
| RMS WFE [nm] | 5 arcmin | 145 | 125 | 132 | 141 |
| | 10 arcmin | 579 | 499 | 528 | 566 |
| PSF FWHM [μm] | $\lambda$ = 5 μm | 24.5 | 21.6 | 21.8 | 21 |
| | $\lambda$ = 30 μm | 146.2 | 129.3 | 130.2 | 125.7 |
| OF [%] | | 3.7 | 5.2 | 4.6 | 4.9 |
| $R_{focal}$ [mm] | | 738 | 778 | 708 | 709 |

**Table 4.** Optical systems prescription for all cases of study.

| | | **Case 1** | **Case 2** | **Case 3** | **Case 4** |
|---|---|---|---|---|---|
| Radius of curvature [mm] | M1 | 7378.909 | 6476.904 | 6360.441 | 6360.441 |
| | M2 | 1725.423 | 1818.414 | 1665.369 | 1665.369 |
| Conic constant | M1 | -1.016404 | -1.023825 | -1.020935 | -1.020679 |
| | M2 | -2.268348 | -2.456266 | -2.40748 | -2.405145 |
| Mirrors CAD [mm] | M1 | 3450 | 3100 | 3100 | 3100 |
| | M2 | 634 | 683 | 639 | 685 |
| Mirrors spacing [mm] | | 2986 | 2511 | 2511 | 2511 |

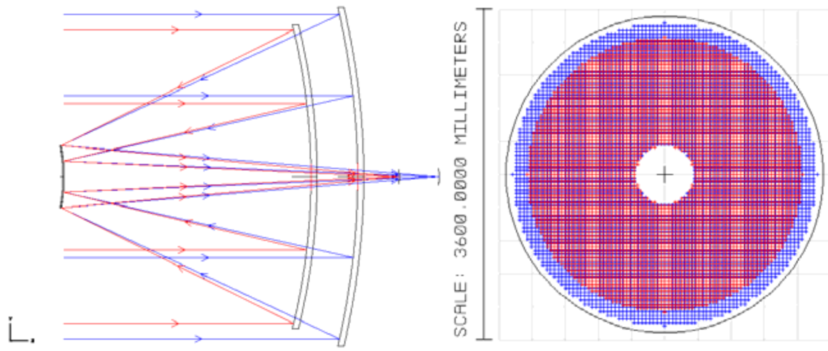


**Fig. 3.** Ray trace on-axis (left) and on-axis beam footprint on M1 (right) for Case 1 (blue) and 3 (red).

V. CONCLUSIONS:

Four different optical designs for the STA were studied and their performance metrics assessed.

From the results of this study it can be concluded that the primary impact of the reduction of the M1 physical diameter from 3.5 m to 3.2 m is a reduction by 18.5% (in worst case, but excluding additional obscuration due to the M2 mounts and spiders) of the STA unobstructed entrance pupil area. The total throughput of the STA is thus reduced by the same amount. The manufacturability of the mirrors is marginally affected. Furthermore, a shorter inter-mirror spacing and smaller M1 diameter is advantageous for the mechanical response of the STA to vibrations and shock loads.

For a given M1 CAD, an increase of the BFL results in larger values for $R_{focal}$ and in larger M2 CAD hence an increase in the M2 mass and of the OF. It is thus recommended to have a BFL as small as possible.

Finally, the position of the stop has little or no impact on the performance metrics. In Case 4 the exit pupil is not physically accessible and this makes the straylight and mirrors thermal self emission more difficult to baffle. The STA stop is therefore chosen to be located on M2.

In view of the results of this study, the STA optical design for Case 3 is the new baseline for further study.

REFERENCES

[1] The SPICA Study Team Collaboration, *SPICA : Revealing the origins of planets and galaxies*, Assessment study report, ESA/SRE(2009)6, arXiv:1001.0709v1, European Space Agency, December 2009.

[2] H. Gross, F. Blechinger, B. Achtner, *Handbook of Optical Systems*, 1st ed., vol.4, Wiley-VCH, pp. 746-750, 2008.

[3] C. du Jeu, “Criterion to appreciate difficulties of aspherical polishing”, *Proc.SPIE Optical fabrication, Metrology, and Material Advancements for Telescopes, United Kingdom*, vol.5494, pp.113-121, June 2004

[4] J.L. Mercier, “Fabrication des composants optiques des engins spatiaux”, *CNES 4eme Journees d’Optique Spatiale de Marseille*, *France*, p.413, November 1973.

[5] J.W. Foreman Jr., “Mercier’s aspheric manufacurability index”, *Applied Optics*, vol.26, iss.22, pp.4711-4712, November 1987.